Clim Dyn (2014) 42:1029–1042
DOI 10.1007/s00382-013-1917-3

Why were some La Niñas followed by another La Niña?

Zeng-Zhen Hu · Arun Kumar · Yan Xue · Bhaskar Jha

Received: 28 September 2012 / Accepted: 11 August 2013 / Published online: 29 August 2013

Abstract This paper investigates why some La Niña events are followed by another La Niña and some others are not. We propose two preconditions that result in continuation of a La Niña. The first one is that La Niña must be a strong event (a major La Niña). This ensures that the reflected Rossby wave signal at the eastern boundary of the Pacific has a strong westward propagating cold ocean temperature anomaly over the off-equatorial region. The off-equator cold anomaly may not be conducive to the equatorial recharge process, and as a result, may favor the persistence of cold ocean subsurface temperature anomaly and prevent the transition from La Niña to El Niño. The second precondition is whether there are eastward propagating downwelling Kelvin waves during the decay phase of a major La Niña. Eastward propagating downwelling Kelvin waves could lead to demise for a tendency for a follow-up La Niña. The equatorial Kelvin wave activities are associated with fluctuations of surface wind in the equatorial far-western Pacific. The analysis suggests that both the surface wind in the equatorial far-western Pacific and the recharge/discharge of the equatorial Pacific are indicators for occurrence or no occurrence of a follow-up La Niña event.

Keywords Multi-year La Nina · Oceanic Kelwin wave · Surface wind stress divergence in far-western Pacific · Recharge and discharge processes

Z.-Z. Hu (✉) · A. Kumar · Y. Xue · B. Jha
NCEP/NWS/NOAA, Climate Prediction Center, 5830 University Research Court, College Park, MD 20740, USA
e-mail: Zeng-Zhen.Hu@noaa.gov

B. Jha
WYLE Science, Technology and Engineering Group, Houston, TX, USA

1 Introduction

As the leading mode of seasonal-to-interannual variability in the tropical climate system, El Niño-Southern Oscillation (ENSO) has significant impacts on global weather and climate anomalies (e.g., Glantz 2000). Interestingly, the El Niño and La Niña, together with their global impacts, are not symmetric in many aspects. For example, tropical sea surface temperature (SST) anomalies (SSTAs) for El Niño and La Niña are asymmetric in their magnitude (Hoerling et al. 1997; Burgers and Stephenson 1999; Okumura et al. 2011; Kumar and Hu 2013), their meridional extension (Zhang et al. 2009), zonal phase propagation (McPhaden and Zhang 2009), and associated atmospheric response and teleconnection patterns (Hoerling et al. 1997).

The temporal evolution associated with El Niño and La Niña events is also not symmetric (Kessler 2002; Kug et al. 2005; Ohba and Ueda 2009; Okumura et al. 2011). Kessler (2002) reported a distinct break in the transition from La Niña to El Niño leading to departure from the concept of ENSO as a cycle. Statistically, after the mature phase, El Niño tends to decay rapidly by next summer, but La Niña event normally persists through the following year, and at times, re-emerges in the subsequent winter, occurring twice or even multiple times over consecutive years. Thus, some La Niñas are followed by another La Niña instead of El Niño as the concept of "ENSO cycle" may warrant.

There have been attempts to explain the asymmetry in the temporal evolution between El Niño and La Niña. Ohba and Ueda (2009) argued that the process responsible for the asymmetry is the nonlinear atmospheric response to SSTs, which originates from the distribution of climatological SST and its seasonal cycle. The atmospheric response to El Niño was shown to go through a rapid reduction (or relaxation) in the eastern Pacific westerly anomalies at the end of boreal winter, leading to thermocline adjustment via generation of eastward propagating upwelling oceanic Kelvin wave (Ohba and Ueda 2009). However, the eastern Pacific easterly anomalies in the cold phase persist into the subsequent spring, and in the absence of rapid change in the surface wind forcing, La Niña SSTAs continue. In addition to the asymmetric atmospheric response to El Niño and La Niña as a cause for their asymmetric temporal evolution, possible influence from the Indian Ocean (Kug et al. 2005; Okumura et al. 2011) has also been proposed as a candidate mechanism. In this hypothesis, the eastward displacement of the convection anomalies during El Niño enables surface winds in the equatorial western Pacific to be more affected by remote forcing from the Indian Ocean leading to a faster termination of the Pacific warm events.

All of the previous work has led to significant progress in the understanding of ENSO mechanisms during the past decade. Nevertheless, significant challenges remain in real-time prediction of different aspects of an ENSO cycle in the state-of-the-art coupled general circulation models (CGCM) (e.g., Guilyardi et al. 2009; Barnston et al. 2012; Kumar and Hu 2012). For example, except for a few models (Zhang et al. 2013), a majority of ENSO prediction models were unable to predict the follow-up La Niña in 2011–2012 (http://iri.columbia.edu/climate/ENSO/currentinfo/archive/index.html). The lack of skill in predicting the follow-up La Niña events was consistent with the observational evidence that during the decay phase of La Niña, recharge of the equatorial Pacific is not robust and equatorial heat content no longer carries the memory of the ENSO cycle forward (Kessler 2002; Kug et al. 2005).

The recharge/discharge of equatorial heat content during an ENSO cycle reflects the oceanic heat exchange between the equator and off-equatorial oceans (Wyrtki 1985; Jin 1997; Wang 2001; Clarke et al. 2007; Wang et al. 2013). During an El Niño, discharge of equatorial heat content occurs and results in heat transportation from the equator to the off-equator. This discharge not only leads to termination of the warm event, but also results in a shallower than normal equatorial thermocline. The anomalous vertical

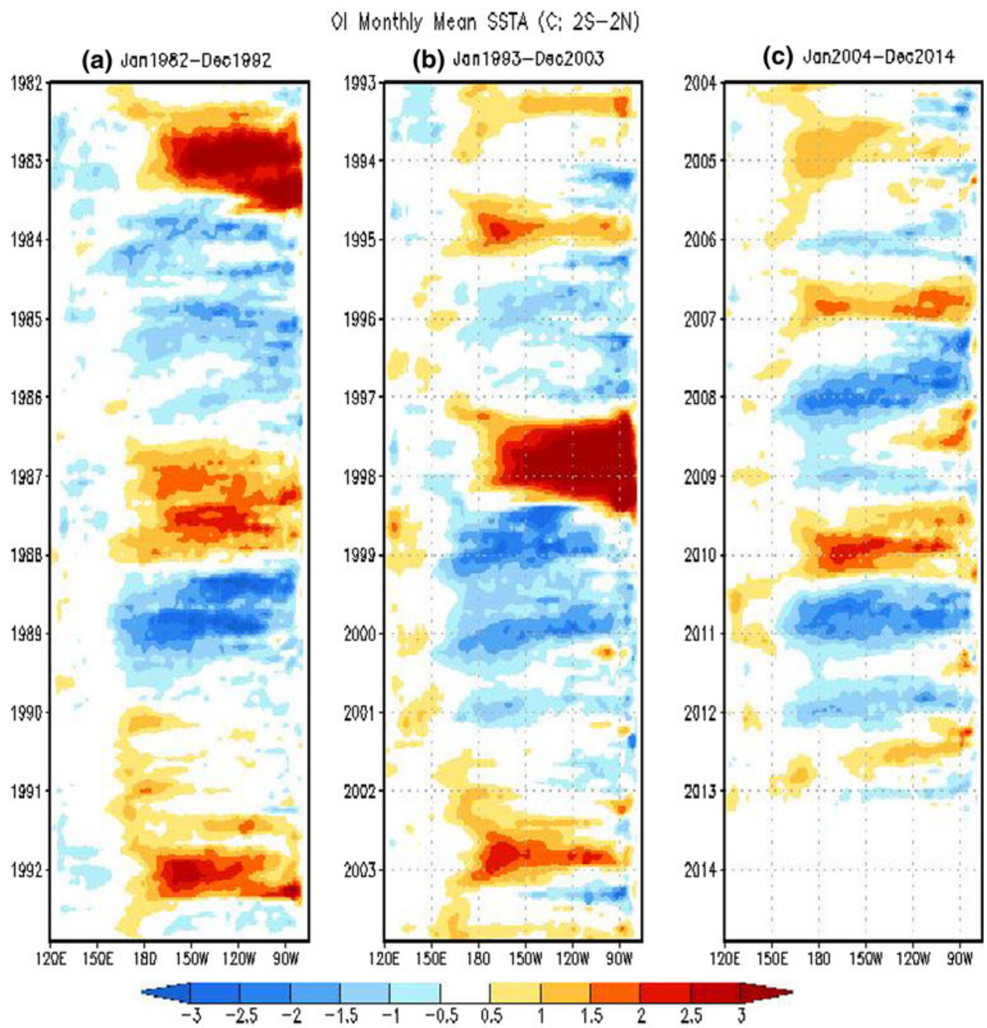

Fig. 1 Monthly mean SSTA averaged between 2°S–2°N and varied with time and longitude: **a** Jan 1982–Dec 1992, **b** Jan 1993–Dec 2003, **c** Jan 2004-Apr 2013. The unit is °C

advection of the colder sub-surface ocean temperature anomalies by mean upwelling (i.e., thermocline feedback), and zonal advection of the mean SST by anomalous westward zonal currents (i.e., zonal advective feedback), lead to La Niña conditions. The reverse happens during a La Niña, reverting the equatorial oceanic conditions back to an El Niño. The recharge/discharge process makes the coupled ocean atmosphere system oscillate on interannual time scales. Details about the recharge/discharge process can be found in Jin (1997), Wang (2001), Clarke et al. (2007), Wang et al. (2013), and references therein.

According to the recharge/discharge mechanism (and other proposed ENSO mechanisms, e.g., delayed oscillator), ENSO is anticipated to be a cyclic oscillation between El Niño and La Niña conditions. However, observed evidence of frequent occurrence of second-year La Niña is a discrepancy from the cyclic behavior of these theories, and its physical mechanism has not been fully understood. For example, 1999–2000 and 2007–2008, 2010–2011 La Niñas are followed by weaker second-year La Niñas, but 1988-89 La Niña was not (Fig. 1). It is expected that through examining the differences between La Niña that are followed or not followed by another La Niña, we may further our understanding in the behavior of ENSO, and eventually improve our predictive ability, and is the focus of this paper.

In this note, using observational data, we analyze the evolution of the oceanic anomalies in the tropical Pacific and the impact of tropical convection and surface winds in the tropical western Pacific in conjunction with the evolution of La Niña in an attempt to understand the differences between La Niña event that is followed by another La Niña and the one that is not. The rest of the paper is organized as follows: we introduce the data used in this work in Sect. 2. The results are shown in Sect. 3, followed by a summary and discussion in Sect. 4.

2 Data

Monthly mean heat content between the ocean surface and 300 m (HC300), monthly and pentad mean depth of 20 °C isotherm (D20), monthly mean surface wind stress, ocean temperature and current, and pentad mean surface wind stress and ocean temperature are from the Global Ocean Data Assimilation System (GODAS) (Behringer and Xue 2004). We also analyze monthly mean warm water volume (WWV index), which was defined as average of D20 in (120°E–80°W, 5°S–5°N) (Meinen and McPhaden 2000).

To measure oceanic Kelvin wave activity, we adopt an oceanic Kelvin wave index, which is defined as standardized projections of GODAS pentad (5-day) mean ocean temperature anomalies (OTAs) onto a first mode of an extended empirical orthogonal function (EEOF). The EEOF is computed using OTAs of the upper 300 meters along the equator between 135.5°E–94.5°W for each 14 contiguous pentad mean from GODAS. The methodology of defining oceanic Kelvin wave index using EEOF with OTAs is similar to that with D20 in Seo and Xue (2005). The index has been used to routinely monitor equatorial oceanic Kelvin wave activity at the Climate Prediction Center (CPC) of National Oceanic and Atmospheric Administration (NOAA) (http://origin.cpc.ncep.noaa.gov/products/people/yxue/ocean_briefing/EDD/OKV_index.gif).

We also utilize observation-based analyses of version 2 of the optimum interpolation (OIv2) monthly mean SST (Reynolds et al. 2002), and outgoing long-wave radiation (OLR) (Liebmann and Smith 1996), both on a 2.5° × 2.5° grid.

All monthly mean data are from Jan 1982-Apr 2013 for the OIv2 SST and Jan 1979-Apr 2013 for the GODAS and OLR data and the pentad mean data are from 03 Jan, 1979–29 Dec, 2011. The climatologies are computed using data from Jan 1982–Dec 2011 for the monthly means and from 1982–2004 using harmonic analysis for the pentad mean data.

3 Results

3.1 SSTA evolution associated with La Niña

We focus on La Niña events after Jan 1982 because of the availability of both OIv2 SST and GODAS data. First, we note that unlike El Niño that normally has a single peak during boreal winter, La Niña events usually have more than one peak in their evolution and extend beyond a single year as depicted by SSTA along the equator (Fig. 1). For example, there were multiple peaks of SSTA for La Niña events occurred in 1983–1986, 1995–1997, 1998–2001, 2007–2009, and 2010–2012, but no multiple peaks for almost all El Niño events during Jan 1982–Apr 2013. This

Table 1 SSTA in the Niño3.4 region averaged in Dec, Jan and Feb (DJF) of the peak years and the following years. The Niño3.4 SSTA is adopted from CPC of NOAA (http://www.cpc.ncep.noaa.gov/products/analysis_monitoring/ensostuff/ensoyears.shtml)

DJF of peak year (SSTA)	DJF of the following year (SSTA)
1984/1985 (−1.0 °C)	1985/1986 (−0.5 °C)
1988/1989 (−1.7 °C)	1989/1990 (0.1 °C)
1995/1996 (−0.9 °C)	1996/1997 (−0.5 °C)
1999/2000 (−1.7 °C)	2000/2001 (−0.7 °C)
2005/2006 (−0.9 °C)	2006/2007 (0.7 °C)
2007/2008 (−1.5 °C)	2008/2009 (−0.9 °C)
2010/2011 (−1.4 °C)	2011/2012 (−0.9 °C)

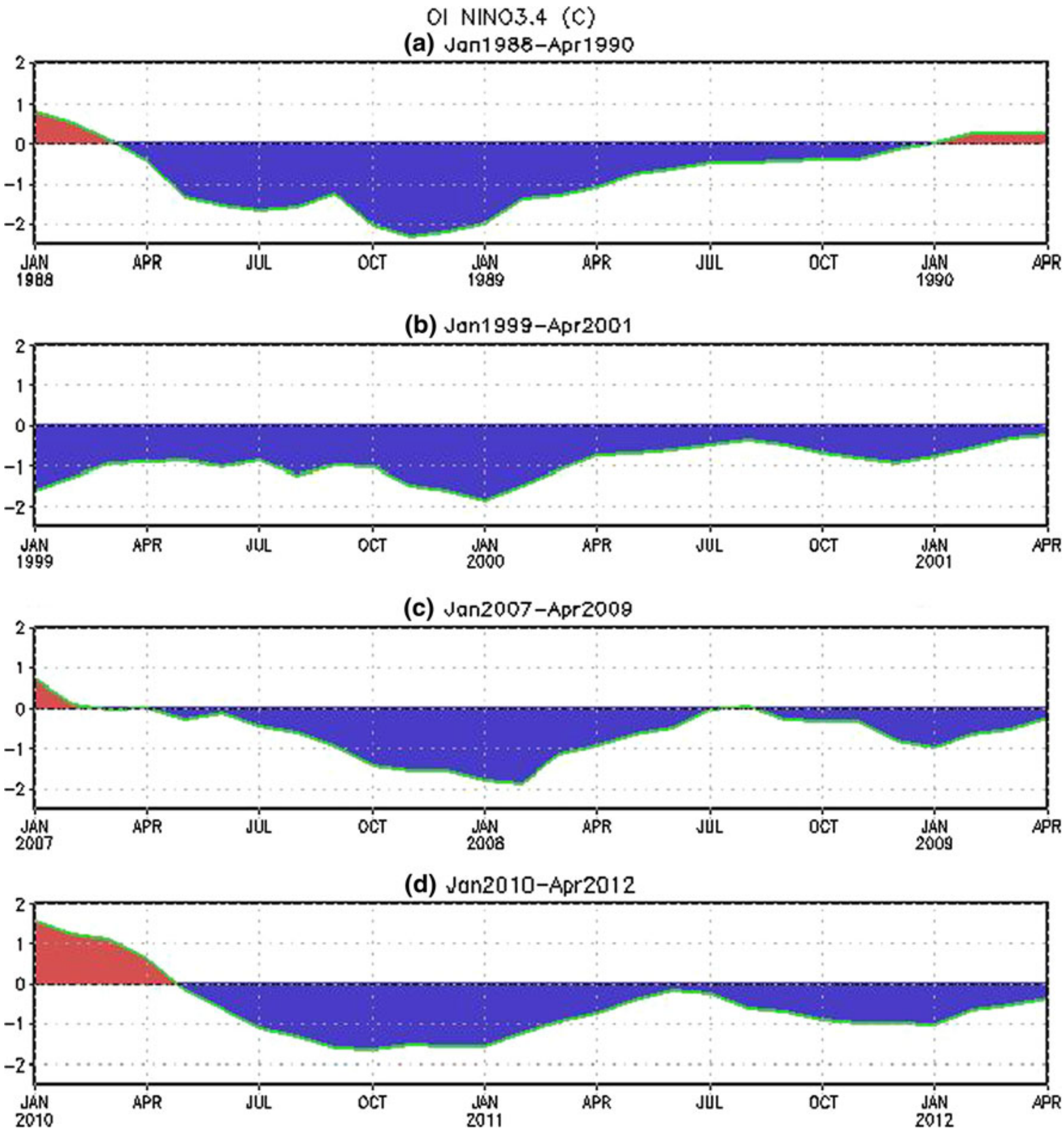

Fig. 2 Monthly mean Niño3.4 index during **a** Jan 1988–Apr 1990, **b** Jan 1999–Apr 2001, **c** Jan 2007–Apr 2009, and **d** Jan 2010–Apr 2012. The index is defined as the SSTA averaged in (5°S–5°N, 170°W–120°W)

asymmetric feature of the SSTA evolution between El Niño and La Niña events has been noted in previous literature (e.g., Kessler 2002; Okumura et al. 2011).

From Fig. 1 and Table 1, we also note that although sometimes the Niño3.4 SST becomes above normal in the following year for some La Niñas, for most La Niñas it remains below normal but with reduced amplitude. After Jan 1982, there were four strong La Niña events with amplitude of monthly mean SSTA averaged in the Niño3.4 region larger than 1.0 °C: 1988–1989, 1999–2000, 2007–2008, and 2010–2011 (Fig. 2, Table 1), and except for 1988–1989, all the other three strong La Niña events were multi-year events. To distinguish the peaks in a multi-year event, we refer to major peak as the first-year La Niña and the post peak as the follow-up La Niña. There are some other La Niña events when amplitude of monthly mean SSTA averaged in the Niño3.4 region was smaller than 1.0 °C, and which are also associated with extended period of negative SSTAs, such as 1984–1986 and 1995–1997 (Fig. 1, Table 1). For these events, the SSTA in the Niño3.4 region doesn't reach −0.5 °C in second peak, and they have not been categorized as multi-year La Niña events following the CPC definition. Thus, the analysis suggests that a strong La Niña is one of the necessary (but not sufficient) preconditions for a La Niña to become a multi-year La Niña event. Possible differences in physical

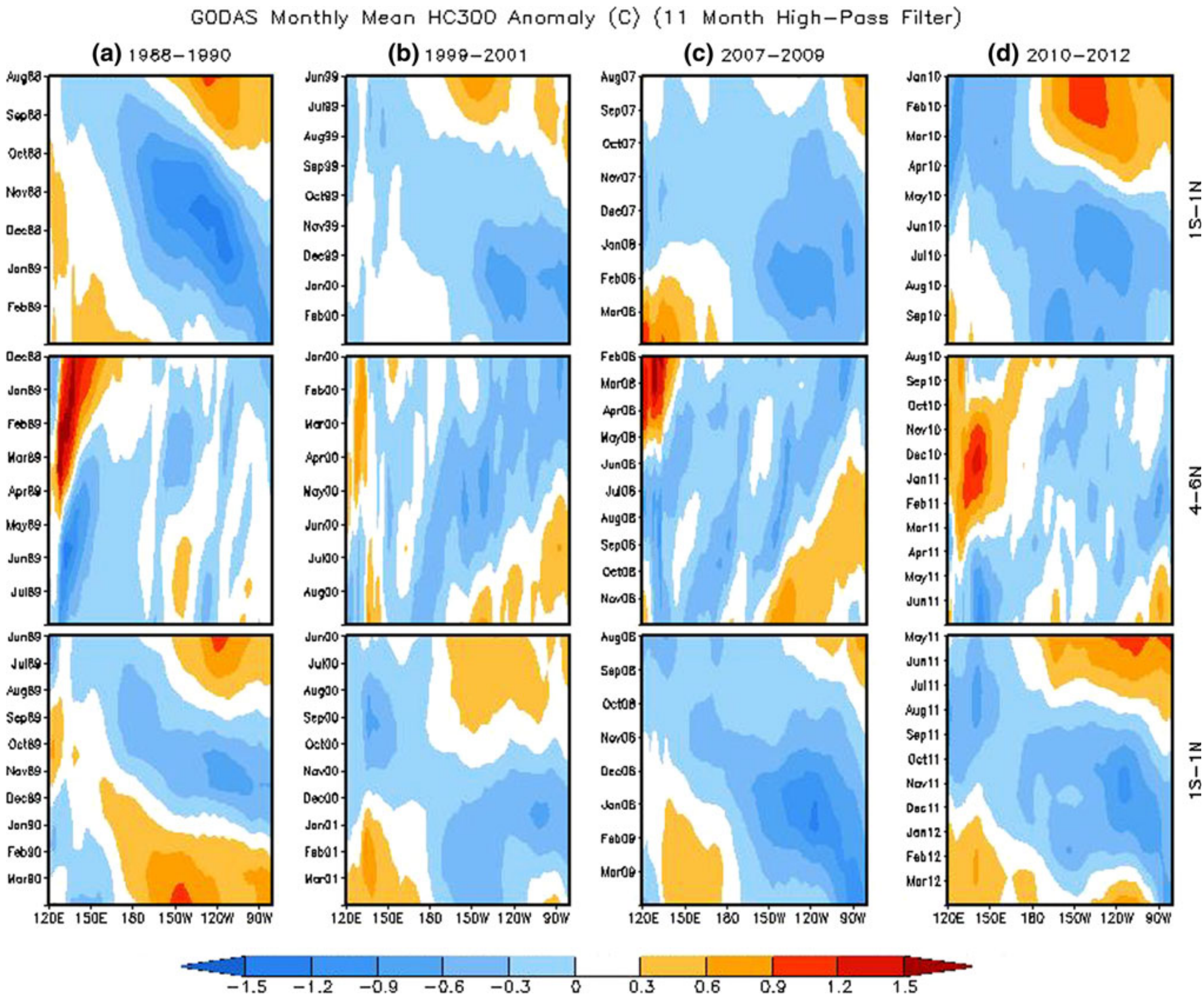

Fig. 3 Monthly mean HC300 anomalies averaged in 1°S–1°N (*top* and *bottom panels*) and in 4°–6°N (*middle panel*) in the Pacific during **a** 1988–1990, **b** 1999–2001, **c** 2007–2009, and **d** 2010–2012. An 11 month high-pass filter is applied to suppress the interannual and longer time scale variations

process linked to the intensity of a La Niña responsible for occurrence and no occurrence of a follow-up La Niña, are discussed next.

3.2 Heat content anomaly propagation and recharge/discharge processes

The linkage of the intensity of a La Niña with the occurrence of follow-up La Niña may be due to the fact that a strong La Niña is likely to ensure that the associated off-equatorial oceanic heat anomalies are strong when they are reflected at the oceanic east boundary and propagate westward as Rossby waves. The stronger westward propagating anomalies have a better chance for maintaining their identity, and create the off-equatorial cold ocean temperature anomalies that may negatively affect the recharge of equatorial heat content, thereby leading to the persistence of cold SST anomalies in the following year.

This speculation is confirmed by the evolutions of HC300 anomalies for the four major La Niña events (Fig. 3). It is seen that pronounced negative HC300 anomalies along the equator accompany all major La Niña events discussed herein (top panels of Fig. 3). Moreover, their eastward propagation or extension along the equator is evident for all four events. The eastward propagating negative HC300 anomaly along the equator reaches the oceanic east boundary in boreal winter (top panels of Fig. 3) at the peak of the major La Niña events (Fig. 2), which is also at the peak of the recharge process (shading in Fig. 4). Subsequently, the negative HC300 anomalies in the oceanic east boundary are reflected as Rossby waves along 4°–6°N (middle panels of Fig. 3) and 4°–6°S (not

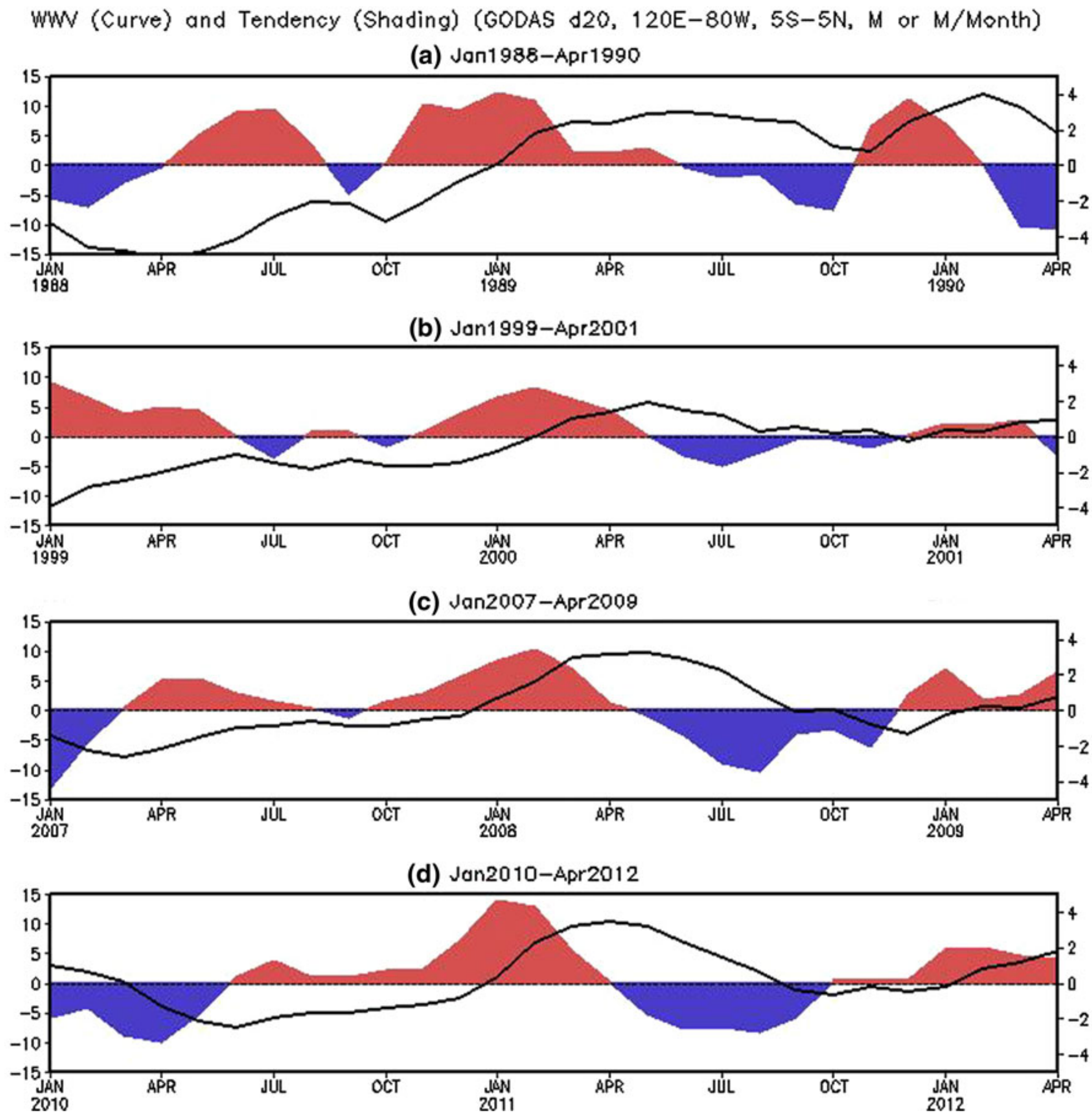

Fig. 4 Same as Fig. 2, but for monthly mean WWV index (*curve*) and its tendency (*shading*). The *y*-axis in the *left* represents the WWV and in the *right* is the WWV tendency. The unit is m for the index and m/month for the tendency

shown) and propagate westward towards the central Pacific in the spring and summer following the first peak of La Niña. Here, the two latitude belts (4°–6°N and 4°–6°S) are chosen based on the HC300 anomaly propagation in the off-equator. Meanwhile, recharge of the equatorial Pacific is halted and is replaced by discharge during the late spring to early autumn, showing negative tendency of WWV anomalies (shading in Fig. 4). Thus, the westward propagating negative HC300 anomalies along the off-equator (middle panels of Fig. 3) may interrupt the recharge process associated with the major La Niña peaks.

The recharge process builds up the equatorial warm water through meridional convergence of Sverdrup transport associated with equatorial central Pacific easterly wind anomalies resulting in a transition to El Niño. For the strong La Niña events, however, the recharge process in spring after the peak is terminated, probably due to the fact that the reflected and westward propagating negative HC300 anomalies along the off-equator results in subsurface ocean temperatures with relatively colder waters than that on the equator. This weakening of recharge process may then prevent transition to an El Niño after major La Niñas. On the contrary, for El Niño events, the equatorial discharge transports heat from the equator to the off-equatorial region (Jin 1997). The equator to poleward heat transport reflects the impact of the equator on the off-equatorial ocean, opposite to the situation of La Niña. This difference may imply that the off-equatorial westward

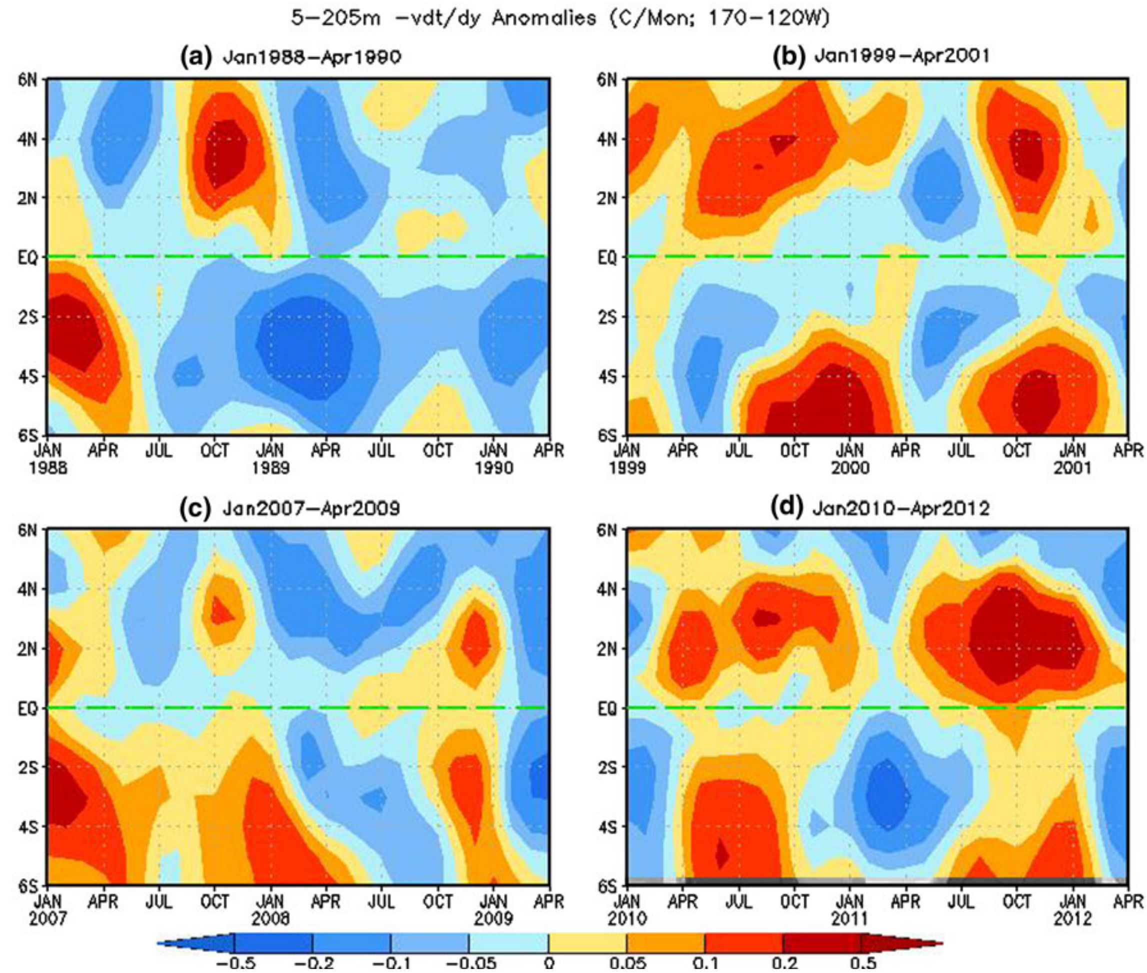

Fig. 5 Meridional ocean temperature advection averaged in 5–205 m and 170°–120°W with unit of °C/month during **a** Jan 1988–Apr 1990; **b** Jan 1999–Apr 2001; **c** Jan 2007–Apr 2008; and **d** Jan 2010–Apr 2012. *Dashed green lines* represent the equator

propagating signals due to the reflection at the oceanic eastern boundary play an important role for occurrence of follow-up La Niña, but not for El Niño, and may be a reason why major La Niña is normally followed by another La Niña, but El Niño is normally not followed by another El Niño (Kessler 2002).

In fact, the overall propagation features of the oceanic heat content anomalies are similar between the weak La Niña events (such as 1984–1986, and 1995–1997, not shown) and the four strong La Niña events (Fig. 3). Although on average, the oceanic heat content anomalies are weaker and the propagation is less obvious for weaker La Niña events, the propagation features shown in Fig. 3 are generally evident for all weak or strong La Niña events.

The evolutions of SSTA and heat content anomalies shown in Figs. 1, 2 and 3 are consistent with those of meridional ocean temperature advection anomalies averaged in 5–205 m and 170°–120°W (Fig. 5). Corresponding to the westward propagation of negative SSTA after the major La Niñas (middle panels of Fig. 3), a cooling tendency in the central and eastern Pacific due to negative meridional ocean temperature advection anomalies is implied in both hemispheres during the first half of 1989 (Fig. 5a), 2000 (Fig. 5b), 2008 (Fig. 5c), and 2011 (Fig. 5d), and may be a factor in halting the recharge during the spring after the major La Niña events (shading in Fig. 4). Thus, the ocean heat propagation and recharge/discharge feature differences provide a physical explanation why La Niña normally is associated with multi-peaks and El Niño has only one peak in their evolution.

The evolution of SSTA shown in Figs. 1 and 2 is also consistent with surface wind stress curl anomaly averaged in 156°E–140°W (Fig. 6) according to Clarke et al. (2007) that cross-equatorial meridional gradient of the surface wind stress curl anomaly is associated with tendency of WWV and Niño3.4 (see their equation 2.20 and Fig. 6). Associated with the peaks of negative SSTA in winter of 1988/1989, 1999/2000, 2000/2001, 2007/2008, 2008/2009,

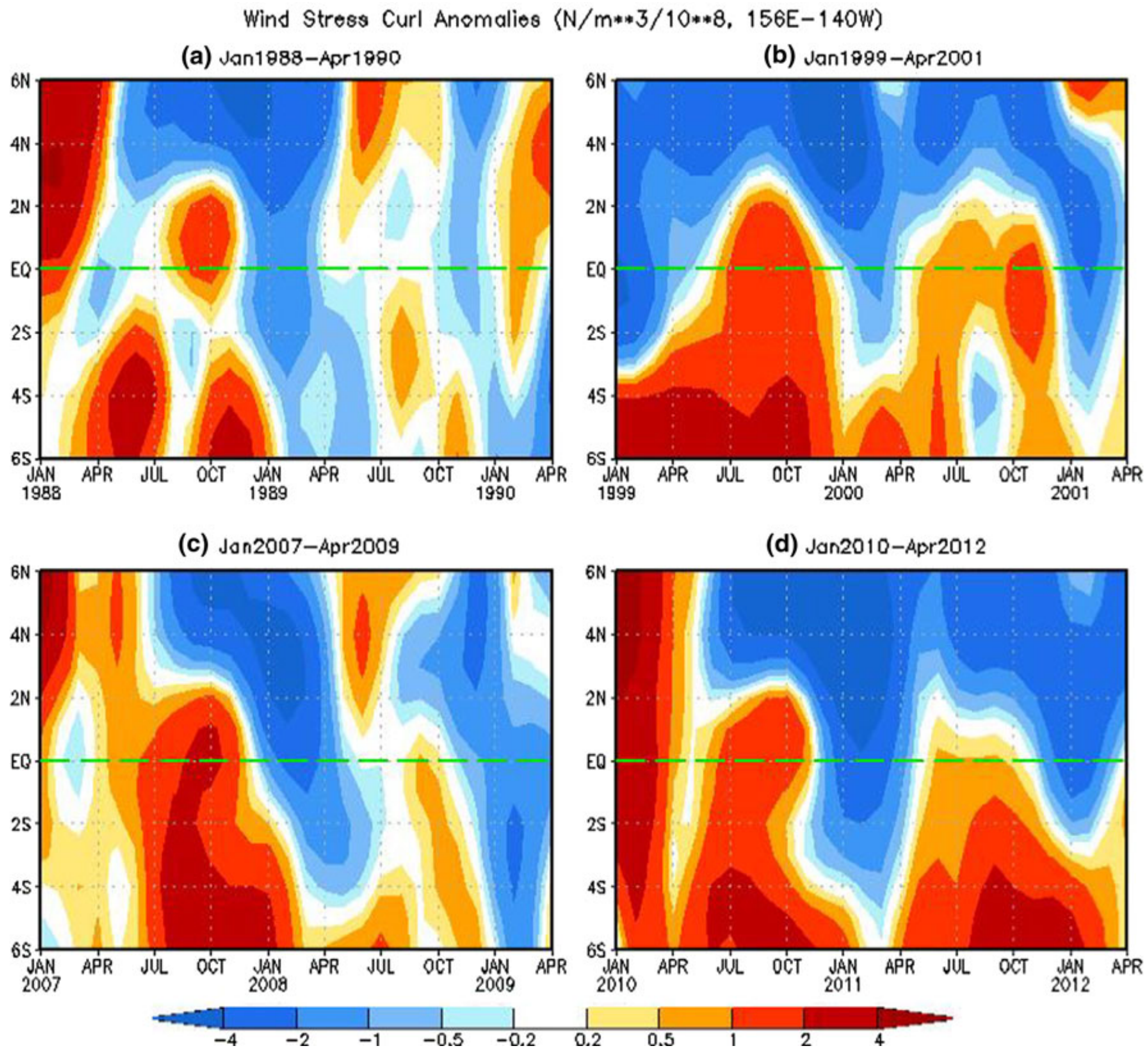

Fig. 6 Surface wind stress curl anomaly with unit of $N/m^3/10^8$ during **a** Jan 1988–Apr 1990; **b** Jan 1999–Apr 2001; **c** Jan 2007–Apr 2008; and **d** Jan 2010–Apr 2012. *Dashed green lines* represent the equator

2010/2011, and 2011/2012 (Figs. 1, 2), strong surface wind stress curl anomaly gradients in the preceding summer to the winter with positive (negative) in the Southern (Northern) Hemisphere are consistent with the regression of surface wind stress curl anomaly onto Nino3.4 index shown by Clarke et al. (2007) (see their Fig. 3). This meridional gradient pattern is caused by anomalous easterly wind in the tropical Pacific with maximum speed around the equator. The negative anomalous wind curl quickly propagates into the equatorial region when the major La Niñas reach their peak. The negative anomalous curl cause increase of WWV as shown in Fig. 4 (shading) because of equatorward convergent meridional flow between the two hemispheres and vortex starching (Clarke et al. 2007).

Besides the qualitative similarities of the ocean heat content anomaly propagation, and the tendency of WWV for the four La Niña events (shading in Fig. 4), there are also some visible differences between the events with and without follow-up La Niña in subsurface OTAs along the equator (bottom panels of Fig. 3) as well as in the WWV itself (curves in Fig. 4). Compared with the other three La Niña events, the equatorial Pacific in the early part of the second year (1989) of 1988–1989 event was warmer. Also, the WWV was above normal, indicating that the thermocline was deeper than the other three La Niña events during this period (see the curves in Fig. 4). The corresponding discharge process ended earlier (Nov 1989), and recharge process was stronger during second half of 1989 and early 1990 (Fig. 4a) compared with the corresponding periods in the other three La Niña events. In addition, the meridional gradient of surface wind stress curl anomaly in second half of 1989 and early part of 1990 (Fig. 6a) is much weaker than that in 2000–2001, 2008–2009, and 2011–2012 (Figs. 6b, c). These differences seem associated with the

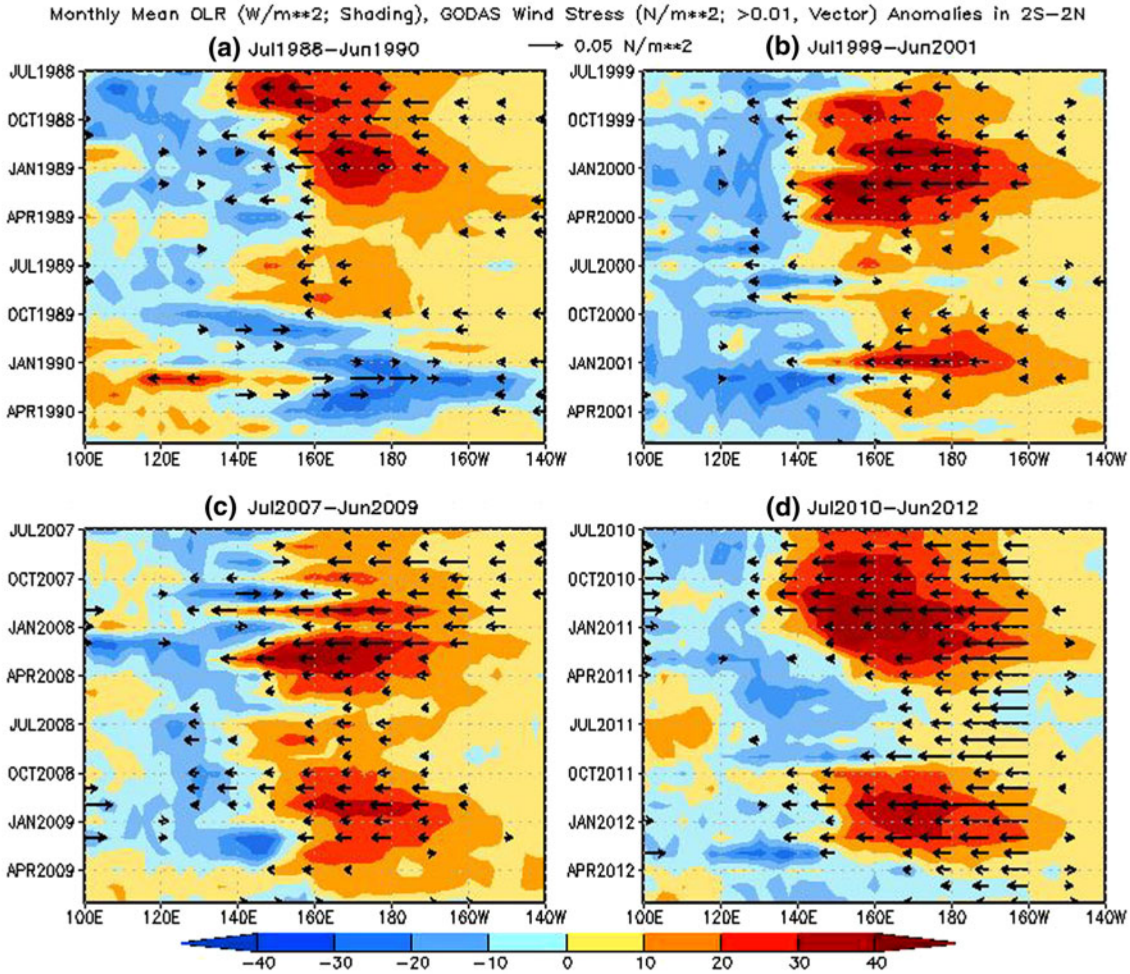

Fig. 7 Zonal component of monthly mean surface wind stress (*vector*) and OLR (*shading*) anomalies along the equatorial Pacific during **a** Jul 1988–Jun 1990, **b** Jul 1999–Jun 2001, **c** Jul 2007–Jun 2009, and **d** Jul 2010–Jun 2012. The zonal wind with speed smaller than 1 m/s is not plotted

differences of Kelvin activity and are discussed in the next subsection.

3.3 Kelvin wave activity and surface wind stress divergence in the equatorial western Pacific

A possible reason for 1988–1990 event to differ from the other three La Niñas is that 1988-90 event had stronger westerly wind anomalies along the equator which are associated with the low-level divergence resulting from suppressed convection in the western Pacific and enhanced convection in the central Pacific in winter of 1989/1990 and early spring of 1990 (Fig. 7a). These anomalies result in eastward propagating downwelling Kelvin wave activities during this period (bottom panel of Figs. 3a, 8a), and together with a deeper thermocline in the equatorial Pacific may have resulted in the demise of the emergence of follow-up La Niña for 1988-89 event. The downwelling oceanic Kelvin wave makes the positive oceanic heat anomalies propagate from the equatorial central Pacific to the eastern Pacific in about 2 months (Fig. 8a). Consistent with the downwelling oceanic Kelvin wave activity, low-level westerly wind anomalies and enhanced convections along the equatorial Pacific are observed and also propagate eastward (Fig. 7a). In contrast, for the other three La Niñas, the surface wind convergence and enhanced convection persisted in the western Pacific and there is no eastward propagating downwelling oceanic Kelvin wave activities (Figs. 7b–d, 8b–d).

The surface wind convergence and convection differences along the tropical Pacific between the event followed and not followed by second-year La Niña shown in Fig. 7 seem associated with the occurrence of Kelvin waves (Fig. 8). To further examine the statistical relation, Fig. 9 shows the correlations of pentad mean anomalies of thermocline slope index with preceding horizontal surface wind stress divergence along the equatorial Pacific. Thermocline slope index is defined as the difference of

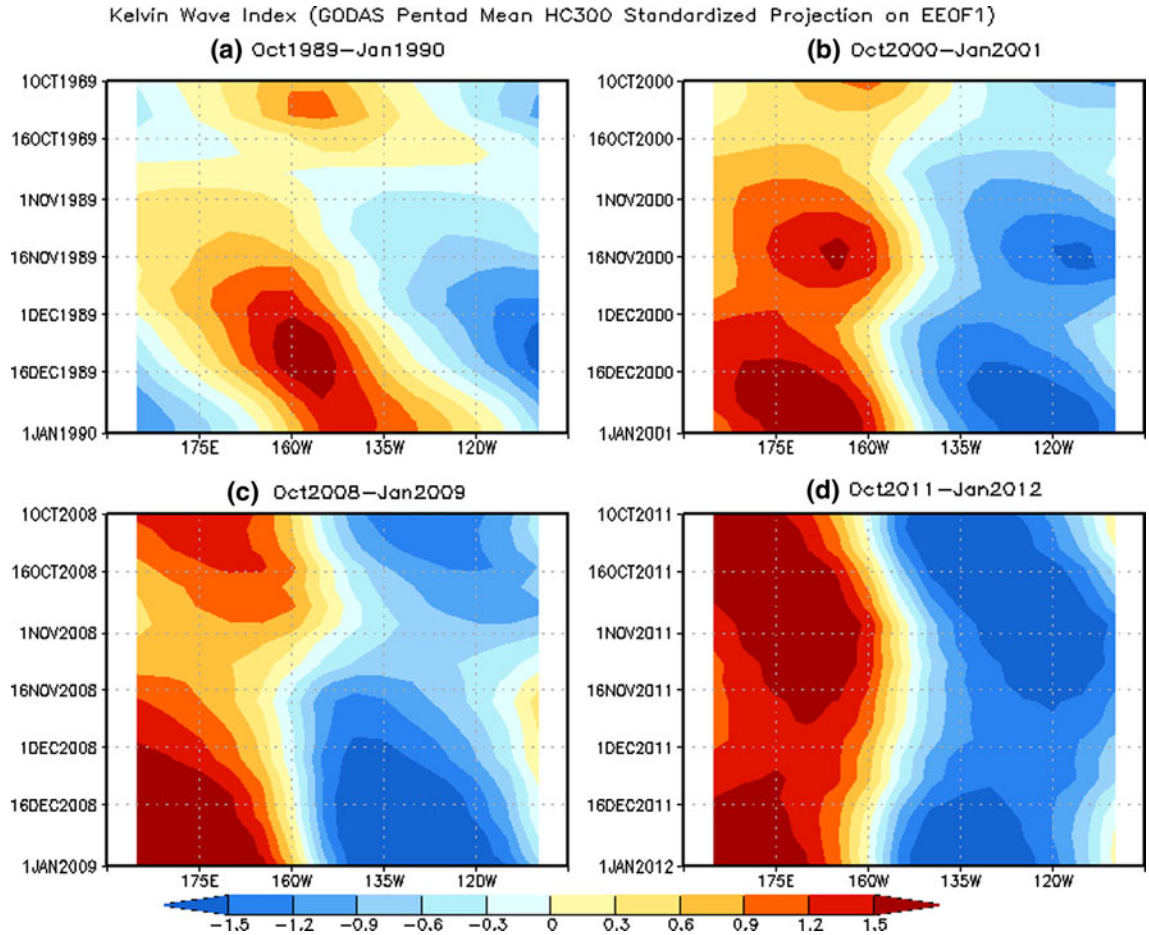

Fig. 8 Standardized projection of pentad mean OTAs along the equator onto 1st mode of EEOF in **a** Oct 1989–Jan 1990, **b** Oct 2000–Jan 2001, **c** Oct 2008–Jan 2009, and **d** Oct 2011–Jan 2012. *X*-axis represents the longitude location of maximum positive loading in the 14 contiguous pentad OTAs of 1st EEOF. See Seo and Xue (2005) for the details of the EEOF calculation

anomalous D20 between the western (160°E–150°W) and eastern (90°–140°W) Pacific (Meinen and McPhaden 2000). Positive (negative) slope index corresponds to negative (positive) phase of ENSO.

A negative correlation is found in the equatorial far-western Pacific around 120°–130°E going back to preceding 320 days (Fig. 9). Negative correlation peaks at about 100–150 days lead and is consistent with the zonal component of surface wind stress anomalies shown in Fig. 7. For the case without follow-up La Niña, the surface wind stress anomalies reversed from easterly to westerly after Oct 1989 (Fig. 7a), while for the cases with follow-up La Niña, the easterly surface wind stress anomalies persisted, and further, enhanced after Oct 2000, Oct 2008, Oct 2011, respectively (Figs. 7b-d). We also note that the zonal surface wind stress anomalies are mainly located to the east of 120°–130°E, that generate the divergence/convergence in the 120°–130°E. Positive correlations are present over the central and eastern Pacific and peak at zero lead. These results suggest that the remote influence of surface wind stress convergence (divergence) in the equatorial far-western Pacific leads the thermocline slope variation by about 3–5 months. Thus, the convergence (divergence) in the equatorial far-western Pacific has the potential to be used as a predictor for the subsequent ENSO evolution (Clarke and Gorder 2001; Kug et al. 2005; Zhang and McPhaden 2010; Wang et al. 2011).

We next investigate the differences of the surface wind stress divergence averaged in the equatorial far-western Pacific (2°S–2°N, 120°–130°E) for the individual La Niña events. The evolution of convergence and divergence in the far-western Pacific was similar for the three La Niña events (Fig. 10b–d), but was different from the 1989–1990 case (Fig. 10a). Using 2007–2009 event as an example (Fig. 10c) for comparison, we note that for 1989–1990 there was no extended period of surface convergence, while persistent and pronounced convergence dominated during Jan 2008–Jan 2009. Extended period of strong convergence in the tropical western Pacific favor the persistency of the cold waters in the

Fig. 9 Correlation between pentad mean surface wind stress divergence anomalies along the equator and the thermocline slope index with the divergence leading the slope index by 400 days to 0 day. The correlation larger than 0.05 is significant at confidence level of 99 % using *t* test

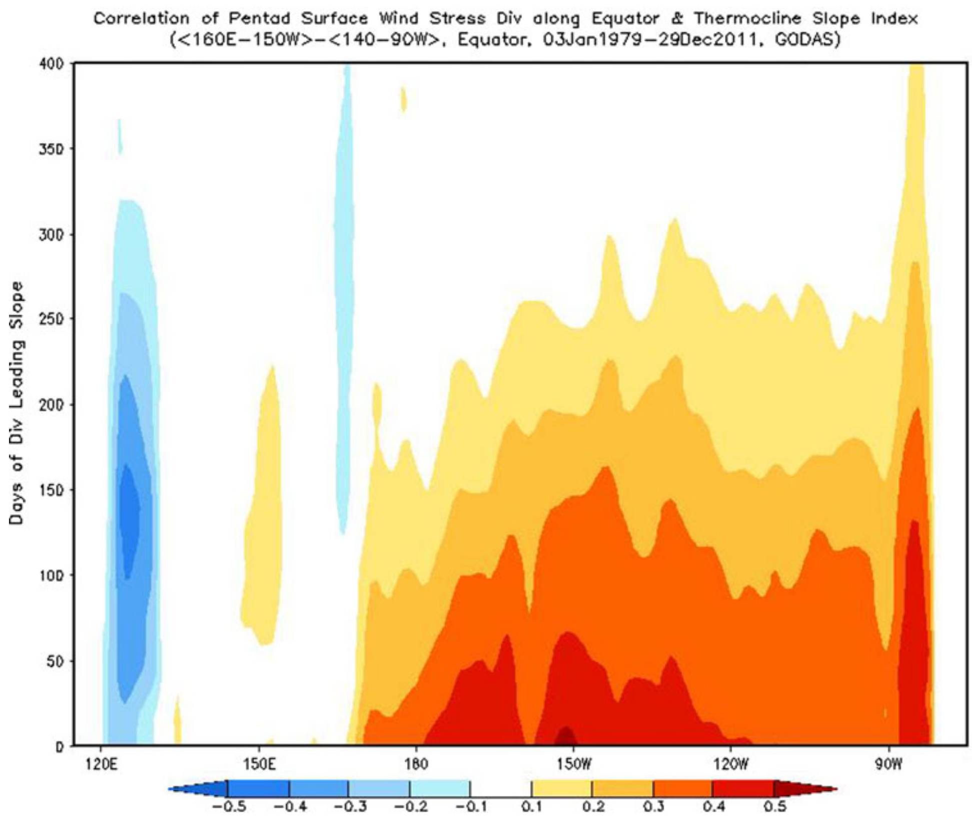

equatorial central and eastern Pacific and the emergence of follow-up La Niña.

In fact, the surface wind stress divergence in the equatorial far-western Pacific is statistically connected with OTA. Figure 11 displays the correlations of pentad mean D20 along the equatorial Pacific with divergence of pentad mean surface wind stress in the equatorial far-western Pacific (2°S–2°N, 120°–130°E). The correlation of wind stress divergence in the western Pacific with D20 gradually increases for both negative anomalies in the west and positive anomalies in the east and propagates eastward in the first 0–100 days, implying a contribution via Kelvin wave activities along the thermocline. Interestingly, correlations increase and reach their peak earlier in the eastern Pacific than in the western Pacific. For example, the correlation reaches its peak when the divergence leads the D20 by 3–4 months in the eastern Pacific and by 5–8 months in the central and western Pacific (Fig. 11). That may suggest that the anomaly in the eastern Pacific is due to fast eastward propagating Kelvin wave and the anomaly in the western Pacific may be caused by some slow processes. Here, we should point out that due to the fact that both regression and correlation are linear analysis, the results shown in Figs. 9 and 11 suggest that thermocline variations associated with both warm and cold ENSO events are connected with surface wind stress in the equatorial far-western Pacific.

The analysis suggests that long persistency of convergence (divergence) in the equatorial far-western Pacific may favor occurrence (not occurrence) of follow-up La Niña. This is consistent with Kug et al. (2005) that the persistence of the western Pacific wind is more important for the onset of El Niño and (major) La Niña than sporadic wind events. The strong convergence in the equatorial far-western Pacific may also favor a continuation of cooling in the equatorial eastern and central Pacific and re-emergence of La Niña. Conversely, weak convergence or divergence in the equatorial far-western Pacific may trigger eastward propagating downwelling Kelvin waves and that may not be conducive for a follow-up La Niña event. This result is in line with Clarke and Gorder (2001) and Kug et al. (2005) who argued that when both equatorial heat content and western Pacific wind are considered together, both the El Niño and La Niña onsets have better predictability.

4 Summary and discussion

In this work, we investigated why some La Niña events are followed by another La Niña (for example, 1999–2001 and 2007–2009, 2010–2012) and some of them are not (for

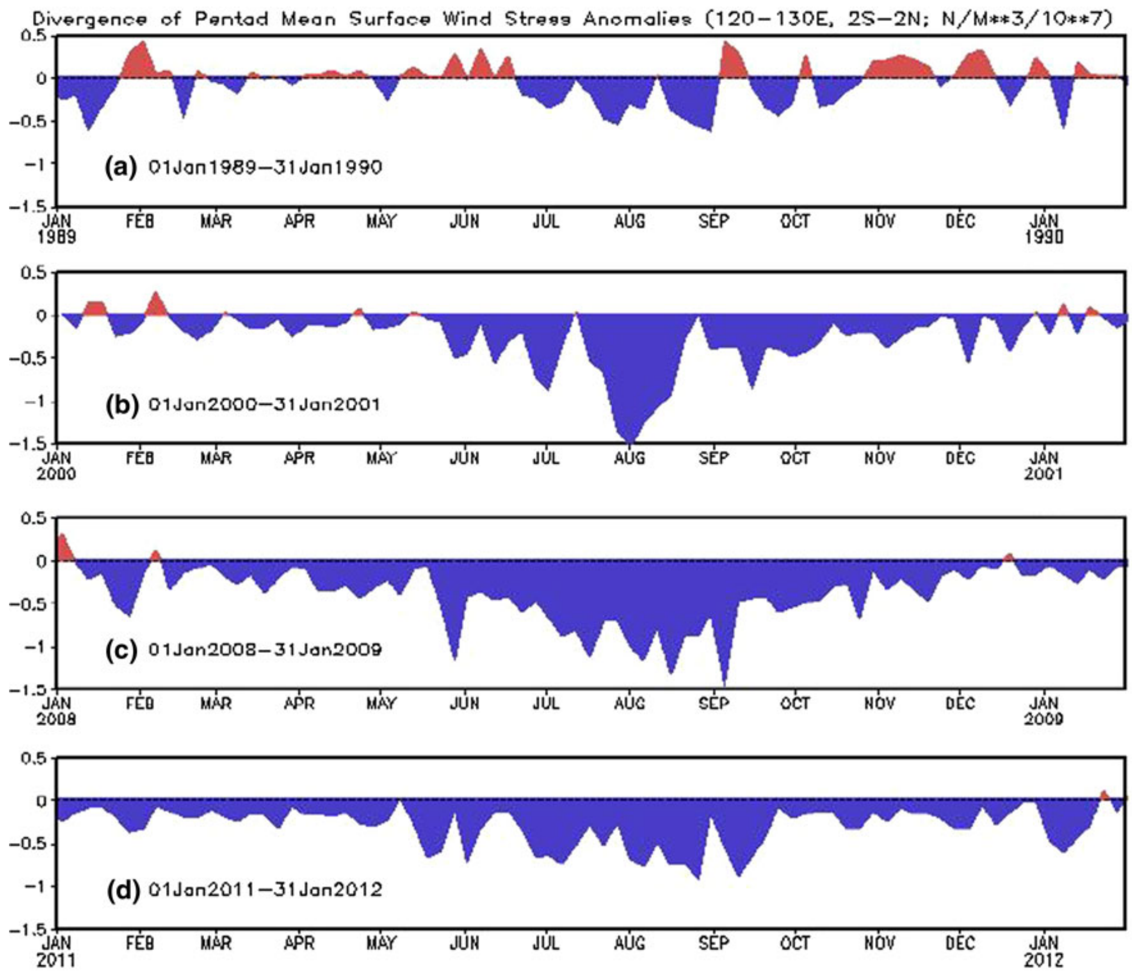

Fig. 10 Divergence of GODAS pentad mean surface wind stress anomalies averaged in 120°–130°E, 2°S–2°N during **a** 01 Jan 1989–31 Jan 1990, **b** 01 Jan 2001–31 Jan 2001, **c** 01 Jan 2008–31 Jan 2009, and **d** 01 Jan 2011–31 Jan 2012. The values are enlarged by 10^7 times with unit N/m^3

example, 1988–1989). We proposed two preconditions to determine whether there will be a follow-up La Niña: (a) A precondition that preceding event is a major La Niña event. This ensures that the reflected Rossby wave signals at the oceanic eastern boundary in the Pacific have a strong westward propagating cold ocean temperature anomaly in the off-equatorial region. The off-equator cold anomaly may interrupt the recharge process and favors the persistence of anomalously cold ocean subsurface and prevent the transition from La Niña to El Niño; (b) Whether there are eastward propagating downwelling warm equatorial Kelvin waves is another precondition to determine if follow-up La Niña occurs or not. Kelvin waves could lead to demise for the tendency for occurrence of a follow-up La Niña.

Our work shows that the Kelvin waves connected to changes in surface winds in western Pacific may determine the continuation or demise of La Nina. The divergence of surface wind anomaly triggers eastward propagating downwelling equatorial Kelvin waves and negative SSTA along the equator Pacific cannot develop further. That results in the termination of follow-up La Niña. Therefore, surface wind anomaly over the equatorial far-western Pacific may provide some clues to monitor and anticipate ENSO evolution (Clarke and Gorder 2001; Kug et al. 2005; Wang et al. 2011).

It is unclear what causes the long-persistent divergence and convergence of surface wind stress anomaly in the equatorial far-western Pacific. The development of Philippine Sea anticyclone (PSAC) argued by Wang and Zhang (2002) may be connected with the surface winds in the equatorial far-western Pacific discussed here. Wang and Zhang (2002) attributed the development of PSAC to combined effects of the remote El Niño forcing, tropical-extratropical interaction, and monsoon-ocean interaction. Thus, the surface wind variability in the equatorial far-

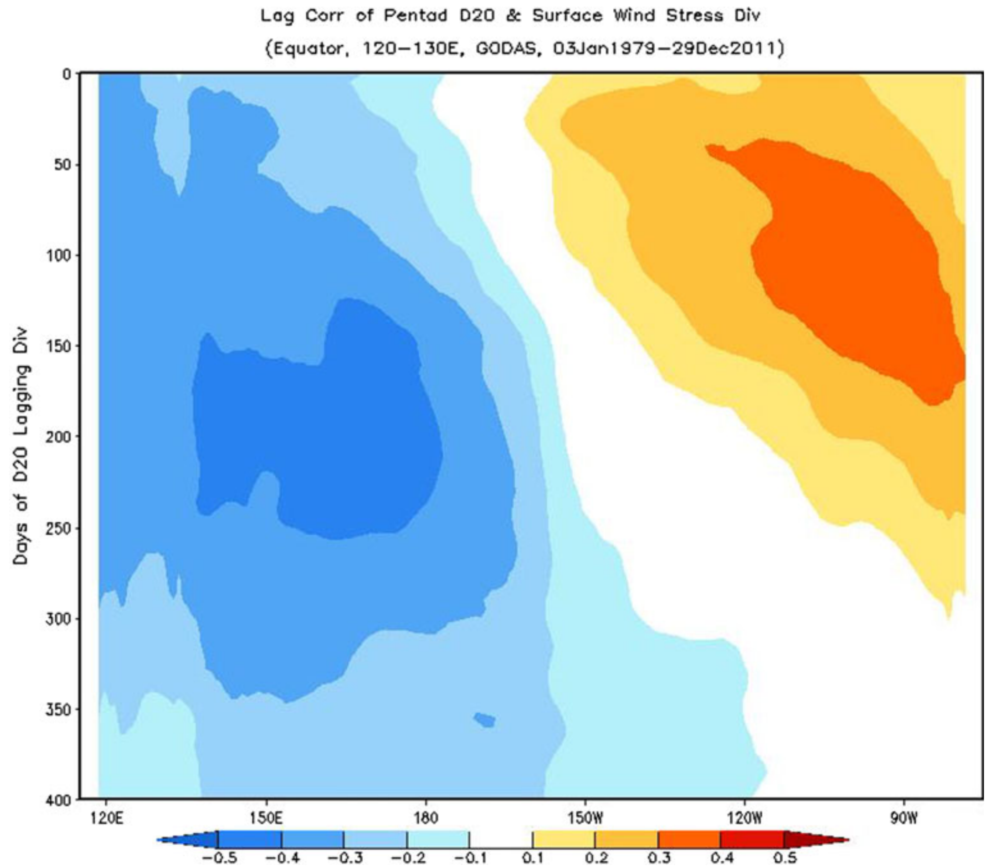

Fig. 11 Correlation between GODAS pentad mean D20 along the equator and GODAS pentad mean surface wind stress divergence anomalies averaged in 120°–130°E, 2°S–2°N during 03 Jan 1979–29 Dec 2011 with the D20 lagging the divergence 0–400 days

western Pacific may be a result of complex physical processes, including feedback from ENSO, East Asian monsoon, and intraseasonal oscillation.

The eastward propagating downwelling warm Kelvin waves might also imply the role played by the Indian and western Pacific Oceans in determining whether there will be a follow-up La Niña. Previous investigations have demonstrated that besides the tropical Pacific, the variation of Indian Ocean also pays an important and active role in affecting the ENSO evolution (Lau and Nath 2003; Annamalai et al. 2010; Kug and Kang 2006). Okumura et al. (2011) suggested that the eastward displacement of atmospheric deep convection anomalies during El Niño enables surface winds in the equatorial western Pacific to be more affected by remote forcing from the Indian Ocean, which acts to terminate the Pacific El Niño events.

While this analysis offered an improved scientific understanding for the ENSO diversity with possible atmospheric and oceanic processes identified based on four historical La Nina cases, however, the implications for more general or more theoretical interests should be investigated further. For example, there is also clear evidence for ENSO modulation and variability on decadal time scales, including the amplitude, oscillation period and propagation characteristics of SSTAs (McPhaden et al. 2011; McPhaden and Zhang, 2009; Lee and McPhaden 2010; Kumar et al. 2010; McPhaden 2012; Hu et al. 2012, 2013). In particular, ENSO behaviors and predictability in the first decade of this century seem to differ from other decades in the last century (Barnston et al. 2012; Hu et al. 2013). Although extensive research has been done over the past three decades, the mechanisms for the modulations of ENSO are still not completely understood. As analyzed in this work, there are clear differences in the La Nina evolution. Do these differences represent decadal changes in ENSO properties (as all three recurring La Niña events were after 1999), or just a random appearance due to the effects of stochastic wind forcing? The relationship between differences in the La Nina evolution and possible decadal modulations of ENSO needs to be further examined. In addition, it should be indicated that due to short length of the data and small sample size used in this work, the robustness of the results needs to be validated using longer observation (reanalysis) data or model simulations.

Acknowledgments This work was stimulated by discussion with Prof. Fei-Fei Jin. We appreciate the comments and suggestions of two reviewers as well as Michelle L'Heureux, Hui Wang, Bohua Huang, and Caihong Wen.

References

Annamalai H, Kida S, Hafner J (2010) Potential impact of the tropical Indian Ocean-Indonesian seas on El Niño characteristics. J Clim 23:3933–3952

Barnston AG, Tippett MK, L'Heureux ML, Li S, DeWitt DG (2012) Skill of real-time seasonal ENSO model predictions during 2002–2011: is our capability increasing? Bull Amer Meteor Soc 93(5):631–651

Behringer DW, Xue Y (2004) Evaluation of the global ocean data assimilation system at NCEP: the Pacific Ocean. Preprints, eighth symposium on integrated observing and assimilation systems for atmosphere, oceans, and land surface, Seattle, WA. Amer Meteor Soc

Burgers G, Stephenson DB (1999) The "normality" of El Niño. Geophys Res Lett 26:1027–1030

Clarke AJ, Gorder SV (2001) ENSO prediction using an ENSO trigger and a proxy for western equatorial Pacific warm pool movement. Geophys Res Lett 28(4):579–582

Clarke AJ, Van Gorder S, Colantuono G (2007) Wind stress curl and ENSO discharge/recharge in the equatorial Pacific. J Phys Oceanogr 37(4):1077–1091

Glantz MH (2000) Currents of change: impacts of El Niño and La Niña on climate and society. Cambridge University Press, Cambridge, p 266, ISBN 052178672X

Guilyardi E, Wittenberg A, Fedorov A, Collins M, Wang C, Capotondi A, van Oldenborgh GJ, Stockdale T (2009) Understanding El Niño in ocean–atmosphere general circulation models: progress and challenges. Bull Amer Meteor Soc 90:325–340

Hoerling M, Kumar A, Zhong M (1997) El Niño, La Niña, and the nonlinearity of their teleconnections. J Clim 10:1769–1786

Hu Z-Z, Kumar A, Jha B, Wang W, Huang B, Huang B (2012) An analysis of warm pool and cold tongue El Niños: air-sea coupling processes, global influences, and recent trends. Clim Dyn 38(9–10):2017–2035. doi:10.1007/s00382-011-1224-9

Hu Z-Z, Kumar A, Ren H-L, Wang H, L'Heureux M, Jin F-F (2013) Weakened interannual variability in the tropical Pacific Ocean since 2000. J Clim 26(8):2601–2613. doi:10.1175/JCLI-D-12-00265.1

Jin F-F (1997) An equatorial ocean recharge paradigm for ENSO. Part I: conceptual model. J Atmos Sci 54:811–829

Kessler WS (2002) Is ENSO a cycle or a series of events? Geophys Res Lett 29(23):2125. doi:10.1029/2002GL015924

Kug J-S, Kang I-S (2006) Interactive feedback between ENSO and the Indian Ocean. J Clim 19:1784–1801

Kug J-S, An S-I, Jin F-F, Kang I-S (2005) Preconditions for El Niño and La Niña onsets and their relation to the Indian Ocean. Geophys Res Lett 32:L05706. doi:10.1029/2004GL021674

Kumar A, Hu Z-Z (2012) Uncertainty in the ocean-atmosphere feedbacks associated with ENSO in the reanalysis products. Clim Dyn 39(3–4):575–588. doi:10.1007/s00382-011-1104-3

Kumar A, Hu Z-Z (2013) Interannual variability of ocean temperature along the equatorial Pacific in conjunction with ENSO. Clim Dyn (online release). doi:10.1007/s00382-013-1721-0

Kumar A, Jha B, L'Heureux M (2010) Are tropical SST trends changing the global teleconnection during La Niña? Geophys Res Lett 37:L12702. doi:10.1029/2010GL043394

Lau N-C, Nath MJ (2003) Atmosphere-ocean variations in the Indo-Pacific sector during ENSO episodes. J Clim 16:3–20

Lee T, McPhaden MJ (2010) Increasing intensity of El Niño in the central equatorial Pacific. Geophys Res Lett 37:L14603. doi:10.1029/2010GL044007

Liebmann B, Smith CA (1996) Description of a complete (interpolated) outgoing long wave radiation dataset. Bull Amer Meteor Soc 77:1275–1277

McPhaden MJ (2012) A 21st century shift in the relationship between ENSO SST and warm water volume anomalies. Geophys Res Lett 39:L09706. doi:10.1029/2012GL051826

McPhaden MJ, Zhang X (2009) Asymmetry in zonal phase propagation of ENSO sea surface temperature anomalies. Geophys Res Lett 36:L13703. doi:10.1029/2009GL038774

McPhaden MJ, Lee T, McClurg D (2011) El Niño and its relationship to changing background conditions in the tropical Pacific Ocean. Geophys Res Lett 38:L15709. doi:10.1029/2011GL048275

Meinen CS, McPhaden MJ (2000) Observations of warm water volume changes in the equatorial Pacific and their relationship to El Niño and La Niña. J Clim 13:3551–3559

Ohba M, Ueda H (2009) Role of nonlinear atmospheric response to SST on the asymmetric transition process of ENSO. J Clim 22:177–192

Okumura YM, Ohba M, Deser C, Ueda H (2011) A proposed mechanism for the asymmetric duration of El Niño and La Niña. J Clim 24:3822–3829. doi:10.1175/2011JCLI3999.1

Reynolds RW, Rayner NA, Smith TM, Stokes DC, Wang W (2002) An improved in situ and satellite SST analysis for climate. J Clim 15:1609–1625

Seo K-H, Xue Y (2005) MJO-related oceanic Kelvin waves and the ENSO cycle: a study with the NCEP Global Ocean Data Assimilation System. Geophys Res Lett 32:L07712. doi:10.1029/2005GL022511

Wang C (2001) A unified oscillator model for the El Niño-Southern Oscillation. J Clim 14:98–115

Wang B, Zhang Q (2002) Pacific-East Asian teleconnection, part II: how the Philippine Sea anticyclone established during development of El Niño. J Clim 15:3252–3265

Wang W, Chen M, Kumar A, Xue Y (2011) How important is intraseasonal surface wind variability to real-time ENSO prediction? Geophys Res Lett 38:L13705. doi:10.1029/2011GL047684

Wang C, Deser C, Yu J-Y, DiNezio P, Clement A (2013) El Niño-Southern Oscillation (ENSO): a review. In: Glymn P, Manzello D, Enochs I (eds) Coral reefs of the eastern Pacific. Springer Science Publisher (in press)

Wyrtki K (1985) Water displacements in the Pacific and the genesis of El Niño cycles. J Geophys Res 90(C4):7129–7132

Zhang X, McPhaden MJ (2010) Surface layer heat balance in the eastern equatorial Pacific Ocean on interannual time scales: influence of local versus remote wind forcing. J Clim 23:4375–4394. doi:10.1175/2010JCLI3469.1

Zhang W-J, Li J-P, Jin F-F (2009) Spatial and temporal features of ENSO meridional scales. Geophys Res Lett 36:L15605. doi:10.1029/2009GL038672

Zhang R-H, Zheng F, Zhu J, Wang ZG (2013) A successful real-time forecast of the 2010–11 La Niña event. Sci Rep 3:1108. doi:10.1038/srep01108